NASA/TM—2013-216515

Advanced Shock Position Control for Mode Transition in a Turbine Based Combined Cycle Engine Inlet Model

Jeffrey T. Csank and Thomas J. Stueber
Glenn Research Center, Cleveland, Ohio

May 2013

NASA STI Program . . . in Profile

Since its founding, NASA has been dedicated to the advancement of aeronautics and space science. The NASA Scientific and Technical Information (STI) program plays a key part in helping NASA maintain this important role.

The NASA STI Program operates under the auspices of the Agency Chief Information Officer. It collects, organizes, provides for archiving, and disseminates NASA's STI. The NASA STI program provides access to the NASA Aeronautics and Space Database and its public interface, the NASA Technical Reports Server, thus providing one of the largest collections of aeronautical and space science STI in the world. Results are published in both non-NASA channels and by NASA in the NASA STI Report Series, which includes the following report types:

- TECHNICAL PUBLICATION. Reports of completed research or a major significant phase of research that present the results of NASA programs and include extensive data or theoretical analysis. Includes compilations of significant scientific and technical data and information deemed to be of continuing reference value. NASA counterpart of peer-reviewed formal professional papers but has less stringent limitations on manuscript length and extent of graphic presentations.

- TECHNICAL MEMORANDUM. Scientific and technical findings that are preliminary or of specialized interest, e.g., quick release reports, working papers, and bibliographies that contain minimal annotation. Does not contain extensive analysis.

- CONTRACTOR REPORT. Scientific and technical findings by NASA-sponsored contractors and grantees.

- CONFERENCE PUBLICATION. Collected papers from scientific and technical conferences, symposia, seminars, or other meetings sponsored or cosponsored by NASA.

- SPECIAL PUBLICATION. Scientific, technical, or historical information from NASA programs, projects, and missions, often concerned with subjects having substantial public interest.

- TECHNICAL TRANSLATION. English-language translations of foreign scientific and technical material pertinent to NASA's mission.

Specialized services also include creating custom thesauri, building customized databases, organizing and publishing research results.

For more information about the NASA STI program, see the following:

- Access the NASA STI program home page at *http://www.sti.nasa.gov*

- E-mail your question to *help@sti.nasa.gov*

- Fax your question to the NASA STI Information Desk at 443–757–5803

- Phone the NASA STI Information Desk at 443–757–5802

- Write to:
  STI Information Desk
  NASA Center for AeroSpace Information
  7115 Standard Drive
  Hanover, MD 21076–1320

NASA/TM—2013-216515

Advanced Shock Position Control for Mode Transition in a Turbine Based Combined Cycle Engine Inlet Model

Jeffrey T. Csank and Thomas J. Stueber
Glenn Research Center, Cleveland, Ohio

National Aeronautics and
Space Administration

Glenn Research Center
Cleveland, Ohio 44135

May 2013

Acknowledgments

The work presented in this paper was funded by the NASA Fundamental Aeronautics Program Hypersonics project. The authors thank Dr. James L. Pittman, NASA Langley Research Center (LaRC), Hypersonics project principal investigator and Mr. Donald I Soloway, NASA Ames Research Center (ARC), Hypersonics project associate principle investigator for controls, for their support and leadership.

This work was sponsored by the Fundamental Aeronautics Program at the NASA Glenn Research Center.

Level of Review: This material has been technically reviewed by technical management.

Available from

NASA Center for Aerospace Information
7115 Standard Drive
Hanover, MD 21076–1320

National Technical Information Service
5301 Shawnee Road
Alexandria, VA 22312

Available electronically at http://www.sti.nasa.gov

Advanced Shock Position Control for Mode Transition in a Turbine Based Combined Cycle Engine Inlet Model

Jeffrey T. Csank and Thomas J. Stueber
National Aeronautics and Space Administration
Glenn Research Center
Cleveland, Ohio 44135

Abstract

A dual flow-path inlet system is being tested to evaluate methodologies for a Turbine Based Combined Cycle (TBCC) propulsion system to perform a controlled inlet mode transition. Prior to experimental testing, simulation models are used to test, debug, and validate potential control algorithms. One simulation package being used for testing is the High Mach Transient Engine Cycle Code simulation, known as HiTECC. This paper discusses the closed loop control system, which utilizes a shock location sensor to improve inlet performance and operability. Even though the shock location feedback has a coarse resolution, the feedback allows for a reduction in steady state error and, in some cases, better performance than with previous proposed pressure ratio based methods. This paper demonstrates the design and benefit with the implementation of a proportional-integral controller, an H-Infinity based controller, and a disturbance observer based controller.

Nomenclature

ADRC	Active Disturbance Rejection Control
AIP	Aerodynamic Interface Plane
CCE	Combined Cycle Engine
CCE-LIMX	Combined Cycle Engine Large-Scale Inlet for Mode Transition Experiments
DMSJ	Dual Mode Scram Jet
HiTECC	High Mach Transient Engine Cycle Code
HSFP	High-Speed Flow-Path
LSFP	Low-Speed Flow-Path
PD	Proportional-Derivative control
PI	Proportional-Integral control
RALV	Reusable Air Breathing Launch Vehicles
TBCC	Turbine Based Combined Cycle

1.0 Introduction

The National Aeronautics and Space Administration (NASA) is interested in technology leading to routine airline-type access to space through the use of Reusable Air Breathing Launch Vehicles (RALV). To achieve this, the Fundamental Aeronautics Program's Hypersonics project was assigned to investigate a Turbine Based Combined Cycle (TBCC) propulsion system for horizontal takeoff and acceleration to hypersonic speeds (Ref. 1). The TBCC propulsion system features a split-flow inlet capable of directing airflow to either or both a turbine engine and dual mode scramjet (DMSJ). One major TBCC objective is the transitioning of thrust production from the turbine engine to the DMSJ, known as mode transition. The technical challenge being addressed in this work is to transition airflow between low speed and high speed flow paths while maintaining inlet performance goals that deliver a required air-flow with tolerable distortion at the turbine engine face, without unstarting the inlet.

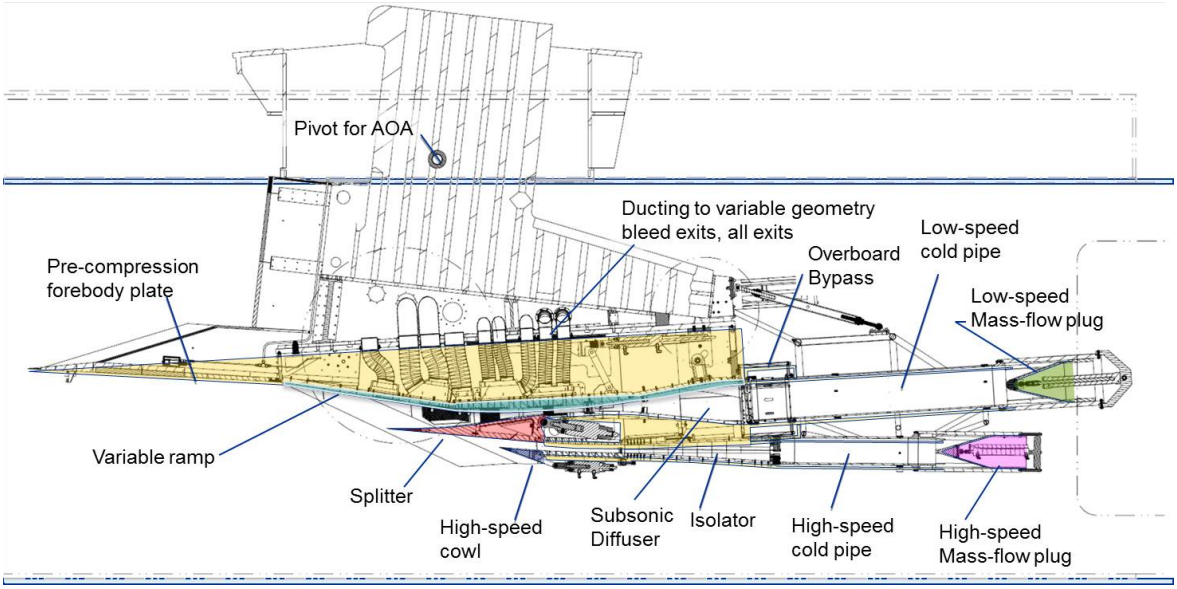

Figure 1.—Diagram of the Combined Cycle Engine Large-scale Inlet for Mode Transition Experiments (CCE-LIMX) in its designed Mach 4.0 configuration with prominent features that pertain to this work identified with labels.

An experimental TBCC system has been designed, built, and mounted in the NASA Glenn Research Center's 10- by 10 Foot Supersonic Wind Tunnel. This inlet is known as the Combined Cycle Engine Large-scale Inlet Model for Mode Transition Experiments (CCE-LIMX) (Ref. 2). A diagram of the CCE-LIMX is shown in Figure 1, as it is mounted in the wind tunnel in the Mach 4 design configuration, with air flow from left to right. As illustrated in Figure 1, air captured by the inlet can be diverted to either an over-mounted low-speed flow-path (LSFP) or under-mounted high-speed flow-path (HSFP) via the splitter. The CCE-LIMX has two cold-pipes with conical mass-flow plugs, which are mounted downstream of the diffuser in the LSFP and downstream of the isolator in the HSFP. The cold-pipe and plug systems are currently used to test the controlled mode transition concept and will be replaced by engines in later phases of testing. Each mass-flow plug can be linearly moved fore or aft, towards or away from cold-pipe close off, to affect the flow path backpressure. For the LSFP, this will simulate the effects from the turbine engine. With wind tunnel air flowing supersonic, using the LSFP mass-flow plug to decrease the cold-pipe exit area will increase backpressure and the static pressure in the subsonic diffuser, moving the normal shock upstream. This course of events is similar to the effect of the turbine engine decreasing power. The LSFP also contains bypass doors, located at the aft end of the diffuser, which can be opened to increase the effective exit area and decrease the diffuser static pressure. A started inlet has the mass-flow plug for the LSFP and bypass doors properly positioned such that the normal shock is aft of the minimum flow path cross sectional area. The location in the LSFP of the minimum cross sectional area is known as the aerodynamic throat and it is located upstream of the diffuser volume. For this work, a started and well controlled inlet will prevent the normal shock from moving upstream of the aerodynamic throat—an unstarted condition.

Airflow disturbances from upstream atmospheric pressure changes or a downstream pressure increase in the diffuser, resulting from the operation of the turbine engine, may cause the shock to naturally move forward of the throat and unstart the inlet. To prevent inlet unstart, the bypass doors can be actively controlled to regulate the static pressure in the diffuser.

When using the diffuser static pressure as a control variable, it is typically normalized with respect to free stream total pressure. Let the term defined as the ratio of the diffuser static pressure to the free stream total pressure be identified as the diffuser pressure ratio. Maximizing this pressure ratio is the main metric of inlet performance. Further opening the bypass doors will continuously decrease the back pressure, and pressure ratio, to maintain the normal shock downstream of the throat and keep the inlet started.

The following are three concerns when operating the bypass doors: First, as the bypass doors open, the normal shock will move further downstream which will result in intolerable distortion at the engine face. Second, opening of the bypass doors will increase the amount of captured air mass that will be vented from the diffuser and back to free stream, essentially increasing the vehicle drag. Third, inlet performance increases as the normal shock moves upstream to the aerodynamic throat, so long as it does not unstart. Therefore, the challenge is to regulate the bypass doors sufficiently to prevent the inlet from unstarting while maximizing inlet performance and minimizing the amount of vented air mass from the diffuser.

The use of bypass doors as an actuator to regulate the pressure ratio and maintain the normal shock in supersonic inlets has been previously shown to be a successful technique (Refs. 3 to 5). Other work has attempted to replace the pressure ratio measurement and use the shock position sensor to provide a more direct measurement of the position of the normal shock (Refs. 4 and 5). The shock position sensor employs an array of pressure measurements located axially down the inlet path in the area of the aerodynamic throat. The location of the normal shock is determined by analyzing the output of the array of sensors to detect an abrupt pressure change due to the shock. Previous work (Refs. 4 and 5) showed that when using the shock position sensor, the disturbed normal shock movement could be attenuated, but only within the resolution of the sensor spacing.

The goal of this work is to develop control algorithms to actively regulate the bypass doors and prevent the inlet from unstarting at the highest possible performance. To reach this goal, potential control algorithms will be implemented and studied using a computation simulation tool that was designed and developed to simulate this type of propulsion system. The simulation tool is known as the High Mach Transient Engine Cycle Code (HiTECC). HiTECC (Ref. 6) is a combined cycle engine (CCE) simulation tool featuring turbine and DMSJ propulsion system models, nozzle models, a heat transfer model, fuel flow models, hydraulics models, etc. The HiTECC tools consist of the following four building blocks, a propulsion system (Ref. 7), a thermal management and fuel system model (Ref. 8), hydraulics and kinematics model (Ref. 9), and finally a control system. The original HiTECC model has been modified to represent the CCE-LIMX (Ref. 10) as it is configured and mounted in the wind tunnel. The modifications included replacing the propulsion system models with a cold pipe and mass-flow plug systems and adding a bypass door at the aft end of the diffuser, as was done experimentally.

With the updated HiTECC model, a closed loop control system has been designed to maintain the normal shock position and prevent inlet unstart in the presence of external disturbances using the pressure ratio as the feedback control variable (Ref. 11). A block diagram of this closed loop control system that regulates the bypass door open area is shown in Figure 2. This closed loop control system consists of a setpoint function, summing junction, controller, plant, and a feedback path. The setpoint function is used to calculate a desired pressure ratio, *r*. The desired pressure ratio is determined from a calculation using free stream conditions and splitter angle as factors. The output of the summing junction is the error signal (*e*) that is a calculated difference between the desired pressure ratio and the plant pressure ratio (*y*). The controller block (*K*) represents where the control algorithm will reside. The plant (*G),* made up of the bypass door and diffuser dynamics, will calculate the feedback signal (*y)* that is applied to the summing junction. In this system, the error and the desired control action are inversely related. To correct this issue, the error signal is multiplied by –1 as shown in Figure 2. If the pressure ratio feedback signal is greater

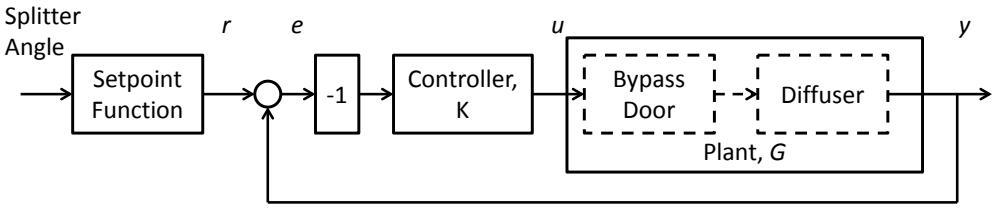

Figure 2.—Closed loop control system using the pressure ratio as the control variable, with an error (*e*) signal applied to the controller (*K*), which produces a bypass door open area command (*u*) applied to the plant (*G*) to produce the desired diffuser pressure ratio output (*y*).

than the setpoint, then the normal shock is further upstream than intended. Increasing the door command will open the bypass doors to decrease the back pressure, ideally returning the feedback signal to the desired level.

With some knowledge of the relationship between the pressure ratio and shock position at various splitter angles, a setpoint function can be designed to apply values to the summing junction that will keep the normal shock safely downstream from the throat. The safe shock position is one that will position the normal shock a little further downstream from the throat than what is necessary to insure that expected fluctuations in diffuser pressure do not unstart the inlet. The potential range of shock movement upstream from the desired shock position that will not result in an unstart is referred to as the operability margin, or stability margin. The goal of the closed loop control system, is to increase inlet performance by allowing a decreased operability margin without compromising the ability to keep the inlet started. The following three control algorithms were designed to be inserted into the controller block in Figure 2 to meet this goal: (Ref. 11) a proportional-integral (PI) controller, H-Infinity based mixed synthesis controller, and disturbance observer based active disturbance rejection control (ADRC) controller. These closed loop controls were computationally demonstrated with the HiTECC tool to be capable of preventing inlet unstarts during a mode transition even while pressure disturbances were being added to the feedback signal. However, these strategies include two major factors which may devalue the capability of the overall closed loop system. The first factor considers the relationship between measured pressure ratio and the ensuing calculated shock position. These calculations have a coarse resolution, thus, adding uncertainty into the closed loop system. The second factor pertains to the actual closing of the splitter. Once activated, the splitter movement is anticipated to close off the LSFP in a continuous negative ramp profile. As the splitter closes, the pressure ratio setpoint will follow the splitter position and it will also decrease. Therefore, if the splitter angle command follows a ramp input pattern, the setpoint function input signal to the closed loop system will also be a ramp pattern. This will result in a steady state error during the mode transition while the splitter is moving.

This paper focuses on modifying the control systems developed in Reference 11 by incorporating a shock position sensor described above and utilizing its output to determine values to be applied to the controller feedback variable. In this work, two types of feedback will be used; first is a continuous signal that measures the position of the normal shock. This is a theoretical sensor with unlimited resolution that can easily be implemented in the HiTECC computational simulation. The second is the limited resolution shock position sensor which can only report the shock position at the first pressure tap location downstream of the actual shock location, similar to what has been used in previous work (Refs. 4 and 5). Section 2.0 discusses modification of the control system to directly accept the shock position feedback signal as the feedback variable. Simulation results and comparison of the same control methods presented in Reference 11 are shown in Section 3.0.

2.0 Shock Position Control With Fixed-Resolution Shock Position Measurement

With the addition of a shock position sensor being used as the feedback variable for the control system of Figure 2, the desired setpoint will be a constant value for all splitter angles. Therefore, the new control system is a modified version of that illustrated in Figure 2 with the exclusion of the setpoint function. Since the goal is to place the shock in a desired position regardless of the control variable, the addition of a shock position sensor should decrease the uncertainty and result in better performance than using a related parameter such as the pressure ratio.

Similar to the approach taken in Reference 11, a linear model of the plant was developed to aid in the control design process. The linear models were developed empirically using the HiTECC tool. The approach taken was to apply a sine-sweep perturbation input signal, starting from a frequency of 0.01 to 50 Hz, to the simulated bypass door actuator and populate a database of bypass door open area and shock position verses time. A step perturbation signal was also applied to the bypass door actuator with the

same amplitude as the sine sweep signal. Next, the sine sweep database was reduced, using the MATLAB *arx* command (provided in the MATLAB System Identification Toolbox), to generate linear models of the bypass door open area to shock position. This process yielded many linear model candidates with varying order. The linear models were tested against the step response data using the MATLAB *compare* function to identify an appropriate model to move forward with. This process netted the following single input single output transfer function that correlates the bypass door open area as the input signal to shock position as the output signal:

$$tf_{SL}(s) = \frac{1000.4(s+56.19)(s^2-505.6s+166400)}{(s+12.12)(s+67.04)(s^2+119.7s+184300)} \tag{1}$$

The subscript *SL* for the transfer function indicates tf_{SL} is a sensitivity function of the shock location measurement to the open area of the bypass doors.

The tf_{SL} transfer function contains right half plane zeroes. Cancellation of right half zeroes is difficult since direct cancellation would require right half plane poles in the controller, which would make the controller transfer function unstable. One method to deal with right half plane zeros is to limit the controller bandwidth to a frequency below the natural frequency of the right half plane zero (Ref. 12). Since the frequency of the right half plane zeroes are quite large, 408 radians per second, limiting the control bandwidth to less than this may be sufficient to avoid the effect of the right half plane zero.

Bode plots of the plant transfer function in Equation (1), which uses the shock location as the controlled variable, are compared to the plant transfer functions given in Reference 11, which uses the pressure ratio as the controlled variable in Figure 3. Assuming that the desired bandwidth and response is below 10 radians per second, these plots show that the shock location plant has more gain and a higher resonant frequency than using the pressure ratio plant; however, the pressure ratio plant has a higher roll off. There is a constant gain offset for all frequencies below 10 radians per second as shown in all of the magnitude plots. In addition, if there is little concern for frequencies above 10 radians per second, then the difference in roll off is of little to no concern. The only remaining concern is the difference in the resonant frequency and the difference is relatively small.

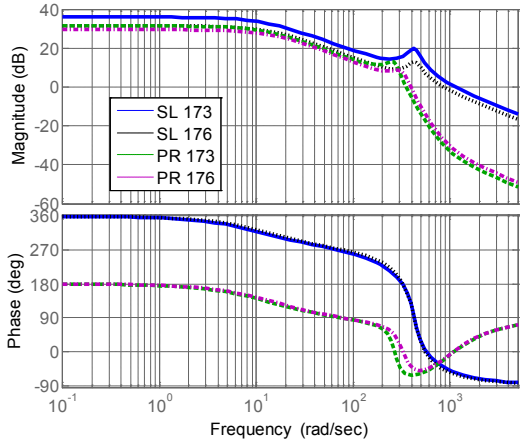

Figure 3.—Bode plot comparing the plant transfer function using the shock location (SL) and pressure ratio (PR) as the feedback variable with the shock located 173 in and 176 in downstream from the tip of the inlet system pre-compression forebody plate.

The simulated shock location sensor employed for this paper was designed to be representative of the shock position sensor in Reference 4. The shock position sensor is implemented as a series of pressure taps aft of the throat. Signal measurements from these sensors were applied to an algorithm that calculated the approximate location of the shock, to the nearest downstream pressure tap. The resolution of this sensor was limited to the spacing between each pressure tap. However, the HiTECC simulation will give an exact location for the normal shock. To simulate this sensor in HiTECC, an additional step was necessary to capture the loss in measured position resolution. An additional look-up table was added to the feedback path in the HiTECC simulation to output the higher position (downstream) value when the normal shock is between two adjacent pressure taps. This implementation approach in HiTECC assumed that there is a pressure tap measurement every inch starting 1 in. upstream from the throat.

3.0 Results and Comparison

This section discusses the implementation of all three closed loop controllers that were designed based on the transfer function identified in Equation (1) to represent the plant with a measured shock location being the controlled variable. The following three controllers being considered are the same three identified in Reference 11: a PI controller, an H-Infinity based mixed synthesis controller, and an active disturbance rejection controller (ADRC). A simulation of these controllers was incorporated into the modified version of HiTECC, as done in previous work (Refs. 10 and 11).

For the mode transition simulations, the splitter will start rotating towards LSFP close-off, a negative angular rotation from the Mach 4.0 design configuration, 0.5 sec after the simulation starts. The splitter will linearly rotate –7.5° in the 0.5 to 2.0 sec simulation window, as shown in Figure 4, which will be used for all simulations in this paper. While the splitter is rotating, the mass flow plug will linearly move 0.25 in. towards cold-pipe close-off to simulate the powering down of the turbine. This span is the critical period. Beyond –7.5°, the bypass doors will be controlled to a fully opened position to maintain supersonic airflow through the throat. This paper assumes fuel flow to the turbine will be terminated, which allows the engine to windmill, when the splitter reaches –7.5° and supersonic flow through the inlet is acceptable. However, unstarting is still not acceptable. While simulating mode transition with the HiTECC tool, commands to change the bypass door open area were added, as shown in Figure 5, to create a disturbance in the diffuser sensors. These disturbances were added to the simulation to determine the susceptibility of the inlet to unstarts while performing a mode transition. These disturbances involved displacements in a bypass door position from fully open to fully closed or vice versa with a frequency response of 20 Hz. The bypass door used to provide the disturbance is referred to as the disturbance door. Prior to applying the initial disturbance, which was an act of closing the disturbance door, the disturbance door was positioned to full open and the exit area of the diffuser was decreased to account for the additional open area of the disturbance door. When decreasing the disturbance door open area, the diffuser pressure will increase which may lead to an unstart. While increasing the disturbance door open

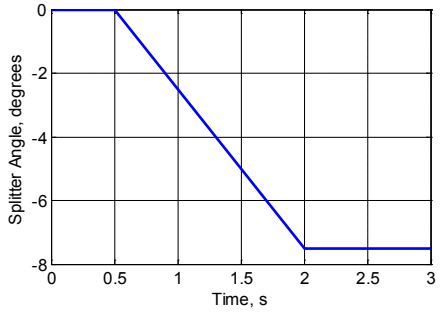

Figure 4.—Splitter command for mode transition in the HiTECC simulation.

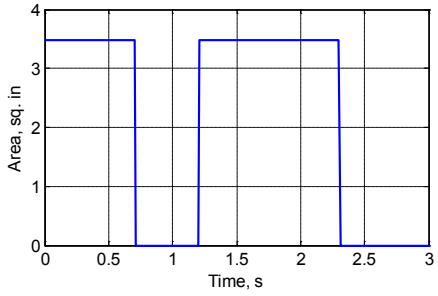

Figure 5.—Disturbance input profile.

area, the diffuser pressure will decrease and the normal shock will move safely away from unstart but towards an inlet operating condition of lower performance. As illustrated in Figure 5, the simulation initiated with the disturbance door open area being set at 3.49 in.^{2} and the mass flow plug was positioned to place the normal shock at a desired location. When the simulation time reached 0.7 sec, the disturbance door open area rapidly decreased to zero. Then, at simulation time 1.25 sec, the disturbance door opened again to 3.49 in.^{2}. Finally, at 2.3 sec, the disturbance door was closed again. Throughout the simulation, another computational bypass door was used to reject the pressure disturbances in the diffuser created by the disturbance door. This door, referred to as the bypass door, received position commands from the controller. The control signal, u, regulates the open area of the bypass door. For these simulations, moving the disturbance door from full open to full closed, without using an active controller to regulate the bypass door, will surely unstart the inlet.

3.1 Proportional-Integral Control

The first control method chosen to implement is the PI controller, where the controller output is:

$$u(t) = k_p e(t) + k_i \int e(t)dt \tag{2}$$

where $e(t)$ is the error ($r(t)$-$y(t)$), and the scalars k_p and k_i are the PI controller gains. The PI controller gains were set to provide the quickest response time with no overshoot, using trial and error PI tuning methods (Ref. 13). For tuning, the continuous feedback measurement (without the limited resolution) was used and the same controller was applied with the limited resolution feedback for an additional comparison. This method proved to provide good results and decreased the tuning effort. The PI controller was chosen to be the baseline for comparison against other controller methodologies because it is the most widely used closed loop controller and because of its intuitive tuning process. The response of the bypass door open area and the normal shock position while using the PI controller, with gains of $k_p = 1.7$ and $k_i = 28$ with a continuous shock position measurement for feedback is shown in the left plots of Figure 6. The right plots in Figure 6 are from a similar simulation, except the feedback signal for the controller was a discrete shock location signal with a resolution of 1 in. For these simulations, the furthest upstream location where the normal shock may reside is at the 161 in. point. If the shock moves upstream of the 161 in. point, the inlet will unstart. This unstart threshold is identified in the lower plots in Figure 6 with a black dotted line. As illustrated in these lower plots in Figure 6, with disturbances applied to the diffuser, while using the PI controller the normal shock remained safely away from unstart. For the

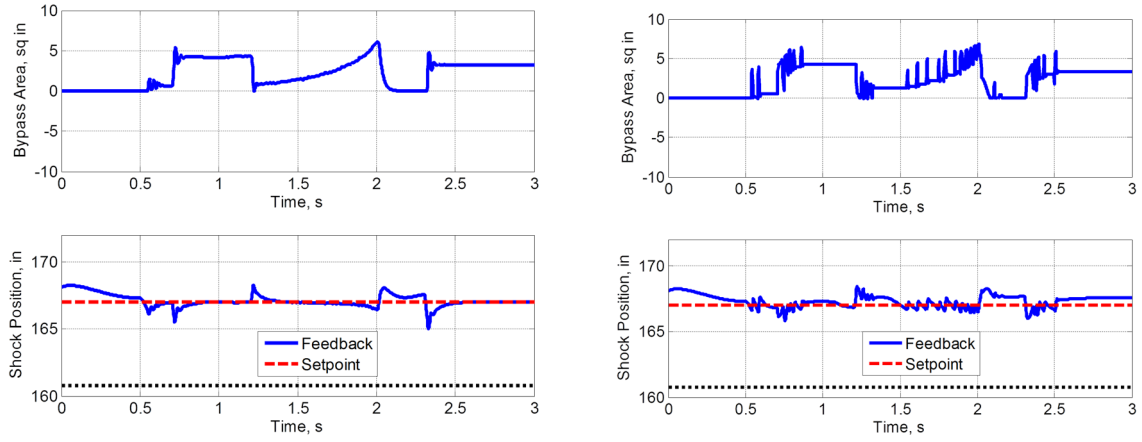

Figure 6.—The bypass door area and shock location using a PI controller and a continuous shock location measurement (left plot) and with a limited resolution shock location feedback signal (right plots).

simulations represented in the left plots, some ringing was observed with the bypass door; however, this ringing was considered acceptable. For the results represented in the right plots, high frequency spikes, or chatter, was recorded during the mode transition due to the limited resolution of the feedback. The limited resolution of the feedback resulted in additional integration, which leads to the high frequency chatter when the error was small. Furthermore, the right side plots include a steady state error at the end of the mode transition due to the limited resolution of the feedback signal.

3.2 Mixed Synthesis Control

The second closed loop controller considered was an H-Infinity mixed synthesis controller. The mixed synthesis controller is an H-Infinity optimal controller that can be designed using the Matlab *mixsyn* command from the Robust Toolbox from MathWorks Inc. The *mixsyn* command computes a state space control law that minimizes the H-Infinity norm for the weighted mixed sensitivity control problem:

$$T_{yu} = \begin{bmatrix} W_1 S \\ W_2 R \\ W_3 T \end{bmatrix} \tag{3}$$

where W_1, W_2, and W_3 are user defined weighting functions. One method for choosing W_1 is to have:

$$W_1 = \frac{\left(s/M\right) + w_B}{s + w_B A} \tag{4}$$

where M is the value of the weighting function W_1 at very high frequencies, A is the value of the weighting function W_1 at steady state, and w_B is the desired bandwidth (10 radians per second). These values can be used as a starting point for determining the weighting function to obtain the desired control performance. Increasing w_B will increase the overall gain of the system and make the response more aggressive. The weighting function W_2 defines the shape of the control input and can be defined as a filter to reduce high frequency spikes from the controller. The weighting function W_3 is typically chosen to be of small magnitude outside the control bandwidth and large inside the control bandwidth which is opposite of W_1.

For this application, after using trial and error tuning methods, the mixed sensitivity weights have been tuned to be:

$$W_1 = \frac{\left(s/50\right) + 160\pi}{s + 0.000088\pi} \quad W_2 = 0.16 \quad W_3 = 0 \tag{5}$$

Defining W_2 as a scalar allows for very fast actuation, which maybe unachievable in actual hardware. In addition, this simulation does not include actuation rate limiters which may allow for high performance than can be achieved in the physical system. Applying these values to the *mixsyn* function resulted in the following closed loop controller transfer function:

$$K_{MS} = \frac{250487.6\left(s + 67.04\right)\left(s + 12.12\right)}{\left(s + 4.322 \times 10^5\right)\left(s + 50.19\right)\left(s + 0.0002765\right)} \tag{6}$$

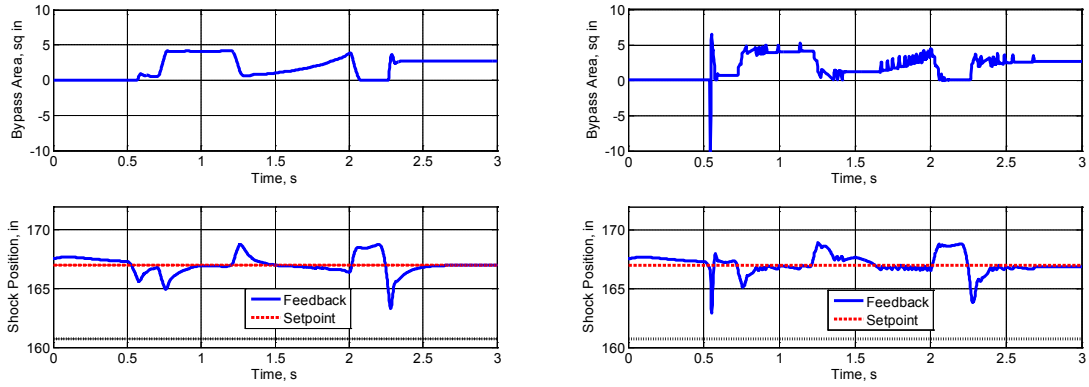

Figure 7.—The bypass door area and shock location response to the mixed synthesis controller with a continuous shock location feedback signal (left plot) and limited resolution shock location feedback signal (right plot).

The response of the inlet using the Mixed Synthesis controller Equation (6) with a continuous shock position signal for feedback is shown in the Figure 7 left plots. The difference between the left and right plots in Figure 7 is the same difference between the left and right plots in Figure 6. The performance of the system when using the feedback signal with the limited resolution, right plots, resulted in a high frequency spike response at the start of the mode transition. This spike in the actuator resulted in a quicker shock position response and overshoot at approximately 0.6 sec (both directions). Note that the minimal open area was 0.0 in.^{2} and the negative area was clipped to 0.0 before being applied to the simulation. Using the mixed synthesis controller, the shock did move closer to the unstart position than with the PI controller; hence, the mixed synthesis controller would require a larger operability margin than with the PI controller.

3.3 Active Disturbance Rejection Control

The final controller is a disturbance observer type controller known as the active disturbance rejection controller (ADRC) (Refs. 14 to 16). The ADRC approach includes a controller and an observer. Details regarding the implementation of the ADRC controller can be found in References 14 to 16.

The ADRC control configuration being considered in this work includes the following three tuning parameters: The DC plant gain, b_0, the controller bandwidth, w_c, and the observer bandwidth w_o. The controller bandwidth is tuned to provide the quickest response time with smallest overshoot. Increasing the controller bandwidth makes the control system response more aggressive. In most applications, the observer bandwidth is set to 10 times the controller bandwidth, but can be tuned manually if needed (Refs. 14 and 15). Usually increasing the observer bandwidth increases the disturbance rejection capability, but sometimes this bandwidth is needed to be limited to filter out high frequency dynamics. Even though the diffuser model of Equation (1) is not a second order plant, the ADRC controller can still be implemented.

The inlet responses with a controlled mode transition using ADRC, with both the continuous and discrete shock location measurements, are shown in Figure 8. Through trial and error tuning efforts, the gains for the ADRC controller were found to be b_0 = 585, w_c = 251.33 rad/sec, and w_o = 2513 rad/sec. The simulation results, when employing the ADRC controller for the process is illustrated in Figure 7. The difference between the left and right plots is the same difference as discussed in the previous two sections. Again, with the discrete feedback signal, the control bypass door response becomes excessively oscillatory.

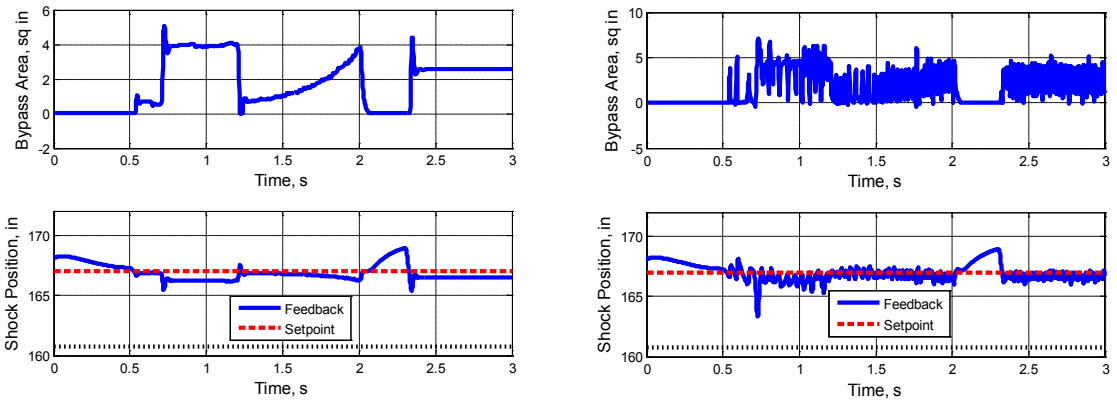

Figure 8.—The bypass door area and shock location response to the Active Disturbance Rejection Control (ADRC) controller for a continuous shock location feedback signal (left plot) and limited resolution feedback signal (right plot).

3.4 Controller Comparison

Three different closed loop controllers have been designed to control the shock position using a continuous shock position feedback signal and a limited resolution shock position feedback signal. There are three closed loop controllers compared in this section: a PI controller, subsection 3.1 and results shown in Figure 6; a mixed synthesis controller, subsection 3.2 and results shown in Figure 7; and ADRC, subsection 3.3 and results shown in Figure 8. Comparing the results with the continuous feedback signal, left hand plots in Figures 6 to 8, the ADRC controller was able to keep the shock furthest downstream of the throat, just slightly better than the PI controller. The PI controller however was able to recover better from the disturbance and return the shock to the setpoint (167 in.) when the disturbance door was closed between a simulation time of 0.7 and 1.2 sec. The mixed synthesis controller, which performed the worst in terms of disturbance rejection and recovery, had the smoothest control signal and least amount of ringing in the control signal. All three controllers were capable of eliminating steady state error during mode transition; something that could not be done in the previous work with HiTECC (Ref. 11).

The results are also compared using the simulation results with the limited resolution feedback signal (1 in.), shown in the right half plots of Figures 6 to 8. With the limited resolution feedback signal, the PI controller clearly provided the best results in terms of disturbance rejection. The mixed synthesis controller and ADRC controllers allowed the shock to move upstream of the 165 point mark and much closer to inlet unstart compared to the PI controller. By limiting the resolution of the feedback, the response of all three systems becomes slightly oscillatory with the ADRC controller being considerably the worst.

This paper shows that with a continuous shock position feedback signal, a controller can be designed using a bypass gate to prevent inlet unstart. The shock position can be more accurately regulated using the continuous shock position feedback signal than what was capable with the previous techniques that used a pressure ratio signal as the feedback signal. However the ability to prevent unstart and disturbance rejection capability degrade as the resolution of the feedback signal decreases. Limiting the resolution of the feedback signal increases the uncertainty and weakens the advantage of this method over previous work using a pressure ratio feedback signal, especially when considering the amount of sensors required to obtain a limited resolution feedback signal. With a pressure tap at every inch starting at the throat and with a resolution of 1 in., 10 sensors would be required for a diffuser (and throat) of 10 in., whereas using the pressure ratio would only require 1 sensor.

4.0 Conclusion

This paper provides alternative closed loop controller designs to prevent an inlet from unstarting during mode transition for Turbine Based Combined Cycle (TBCC) propulsion systems. These controllers employed both shock position measurement sensors and shock position estimator sensors as the controller feedback. All three closed loop controllers were implemented in the High Mach Transient Engine Cycle Code (HiTECC) simulation designed to simulate the combined cycle engine large-scale inlet for mode transition experiments (CCE-LIMX). Previous work demonstrated that with an approximate (estimated) relationship between shock position location and diffuser pressure ratio, a closed loop system can be designed to regulate shock position location by actually controlling the diffuser pressure ratio. In this paper, the control system is modified to use simulated direct measurement of shock position location via a theoretical, high-resolution, sensor as well as a limited-resolution sensor that utilizes multiple pressure sensors located axially in the inlet throat. Using the ideal (high resolution) shock location measurement all three control systems eliminated the steady state error during mode transition. Additionally, all three proposed controllers, Proportional-Integral, H-Infinity based Mixed Synthesis Controller, and the Active Disturbance Rejection Controller were able to prevent inlet unstart even in the presence of large pressure disturbances. However, when the feedback signal was modified to a limited resolution, the performance of the three controllers decreased, mainly due to high frequency oscillations in the feedback signal. Although a determination of the lower bound of resolution for direct shock position measurement was not achieved this report clearly indicates that having a sensor that directly measures shock position can result in better system performance, i.e., higher pressure ratio and a tighter shock position control margin.

References

1. Stueber, T.J., Csank, J.T., Thomas, R., and Vrnak, D.R., "Dynamic Models for the NASA Combined Cycle Engine Large Scale Inlet," Joint Army-Navy-NASA-Air Force (JANNAF), Monterey, CA, December 3–7, 2012.
2. Sanders, B.W., and Weir, L.J., "Aerodynamic Design of a Dual-Flow Mach 7 Hypersonic Inlet System for a Turbine-Based Combined-Cycle Hypersonic Propulsion System," NASA/CR—2008-215215, June 2008.
3. Neiner, G.H., Crosby, M.J., Cole, G.L., "Experimental and Analytical Investigation of Fast Normal Shock Position Controls for a Mach 2.5 Mixed-Compression Inlet," NASA TN D-6382, July 1971.
4. Cole, G.L., Neiner, G.H., Crosby, M.J., "Design and Performance of a Digital Electronic Normal Shock Position Sensor for Mixed-Compression Inlets," NASA TN D-5606, December 1969.
5. Baumbick, R.J., Neiner, G.H., Cole, G.L., "Experimental Dynamic Response of a Two-Dimensional, Mach 2.7 Mixed-Compression Inlet," NASA TN D-6957.
6. Haid, D.A., and Gamble, E.J., "Integrated Turbine-Based Combined Cycle Dynamic Simulation Model," 58th Joint Army-Navy-NASA-Air-Force (JANNAF) Interagency Propulsion, Arlington, VA, April 18–22, 2011.
7. Gamble, E.J., Haid, D., D'Alessandro, S., and DeFrancesco, R., "Dual-Mode Scramjet Performance Model for TBCC Simulation," AIAA–2009–5298, August 2009.
8. Gamble, E.J. and Haid, D., "Thermal Management and Fuel System Model for TBCC Dynamic Simulation," AIAA–2010–6642, July 2010.
9. Gamble, E.J. and Haid, D., "Hydraulic and Kinematic System Model for TBCC Dynamic Simulation," AIAA–2010–6641, July 2010.
10. Csank, J.T., and Stueber, T.J., "A Turbine Based Combined Cycle Engine Inlet Model and Mode Transition Simulation Based on HiTECC Tool," AIAA–2012–4149, 48th AIAA/ASME/SAE/ASEE Joint Propulsion Conference and Exhibit, Atlanta, GA, July 31-August 1, 2012.
11. Csank, J.T., Stueber, T.J., "Shock Position Control for Mode Transition in a Turbine Based Combined Cycle Engine Inlet Model," JANNAF 2012.

12. Skogestad, S., and Postlethwaite, I., "Multivariable Feedback Control: Analysis and Design," John Wiley & Sons, Ltd., West Sussex, England, 1996.
13. Åström, K. and Hägglund T., "PID Controllers: Theory, Design, and Tuning," 2nd Edition, Instrument Society of America, Research Traingle Park, NC, 1995.
14. Gao, Z., "Active Disturbance Rejection Control: A Paradigm Shift in Feedback Control System Design," American Control Conference, Minneapolis, Minnesota, June 14–16, 2006.
15. Gao, Z., Huang, Y., and Han, J., "An Alternative Paradigm for Control System Design," IEEE Conference on Decision and Control, 2001.
16. Gao, Z., "Scaling and Bandwidth-Parameterization Based Controller Tuning," American Control Conference, Denver, CO, June 2003.